

Earth's Future



RESEARCH ARTICLE

10.1029/2023EF003754

Key Points:

- The effect of May North Pacific Oscillation (NPO) on summer rainfall at Northeast China (NEC) is not stable, with a strong (weak) relation for 1986–2010 (for 1961–1985 and 2011–2020)
- This is attributed to a stronger Rossby wave source stimulated by NPO during 1986–2010 than during 1961–1985 and 2011–2020
- The strengthened Rossby wave related with NPO is attributed to the intensification of NPO and to the enhanced relation between NPO and North Atlantic Oscillation

Supporting Information:

Supporting Information may be found in the online version of this article.

Correspondence to:

B. Zhou,
zhoubt@nuist.edu.cn

Citation:

Han, T., He, S., Zhou, B., Li, S., & Hao, X. (2023). Interdecadal changes in the linkage between North Pacific Oscillation during May and Northeast China precipitation during mid-summer: The influence of North Atlantic Oscillation. *Earth's Future*, 11, e2023EF003754. <https://doi.org/10.1029/2023EF003754>

Received 21 APR 2023
Accepted 18 OCT 2023



Author Contributions:

Conceptualization: Shengping He, Shangfeng Li, Xin Hao
Formal analysis: Tingting Han
Investigation: Tingting Han
Methodology: Tingting Han, Shengping He
Project Administration: Botao Zhou
Resources: Botao Zhou
Software: Tingting Han
Supervision: Botao Zhou

© 2023 The Authors.

This is an open access article under the terms of the [Creative Commons Attribution-NonCommercial License](https://creativecommons.org/licenses/by/4.0/), which permits use, distribution and reproduction in any medium, provided the original work is properly cited and is not used for commercial purposes.

Interdecadal Changes in the Linkage Between North Pacific Oscillation During May and Northeast China Precipitation During Mid-Summer: The Influence of North Atlantic Oscillation

Tingting Han^{1,2} , Shengping He^{3,4} , Botao Zhou^{1,2} , Shangfeng Li⁵, and Xin Hao^{1,2} 

¹Collaborative Innovation Center on Forecast and Evaluation of Meteorological Disasters/Key Laboratory of Meteorological Disaster, Ministry of Education, Nanjing University of Information Science and Technology, Nanjing, China, ²Nansen-Zhu International Research Centre, Institute of Atmospheric Physics, Chinese Academy of Sciences, Beijing, China, ³Geophysical Institute, University of Bergen and Bjerknes Centre for Climate Research, Bergen, Norway, ⁴Nansen Environmental and Remote Sensing Center, Bergen, Norway, ⁵Jilin Provincial Key Laboratory of Changbai Mountain Meteorology & Climate Change, Laboratory of Research for Middle-High Latitude Circulation Systems and East Asian Monsoon, Institute of Meteorological Sciences of Jilin Province, Changchun, China

Abstract Many previous studies have documented the relationship between the North Pacific Oscillation (NPO) and the weather/climate of upstream and downstream regions. However, the stability of NPO precursor signals of East Asian summer precipitation, which is important for climate prediction, has received little attention. This study identified temporal variations in the connection between the May NPO and subsequent midsummer precipitation over Northeast China (NEC) during 1961–2020. During 1986–2010, the correlation between the May NPO and midsummer precipitation over NEC was found significantly positive, whereas the relation was found statistically insignificant during 1961–1985/2011–2020. Further results indicated that the NPO stimulated a Rossby wave source over the North Pacific that was stronger during 1986–2010 than during 1961–1985/2011–2020. The Rossby wave source anomalies shifted to North America and to the North Atlantic during the subsequent June and midsummer, respectively. Consequently, a teleconnection wave train, which originated over the North Pacific, propagated eastward to North America, across the North Atlantic, and on to East Asia on the subseasonal time scale, influencing midsummer precipitation over NEC through modulation of the atmospheric circulation (e.g., horizontal wind, moisture transport, and vertical movement). Moreover, the intensified Rossby wave anomalies associated with the May NPO were attributed to the strengthened NPO, which could be related to the enhanced standard deviation of SLP over the North Pacific. Additionally, the strengthened out-of-phase relation between the NPO and the North Atlantic Oscillation, resulting from changes in the background circulation, partially contributed to intensification of the Rossby wave train.

Plain Language Summary The North Pacific Oscillation (NPO) is an important intrinsic atmospheric variability which is characterized by a north–south seesaw in sea level pressure over the North Pacific Ocean. The NPO has substantial influences on the weather/climate conditions over North America and East Asia. However, the relation between NPO and East Asian climate is not stationary. This study identified a temporal variation in the connection between the May NPO and the midsummer precipitation over Northeast China (NEC) during 1961–2020, which shows a strong (weak) correlation during 1986–2010 (1961–1985 and 2011–2020). This is attributed to the different atmospheric circulation patterns caused by the NPO during the three periods. The NPO can simulate stronger perturbation to the atmosphere during 1986–2010 than during 1961–1985 and 2011–2020. Consequently, the perturbed atmospheric waves can propagate eastward to North America, across the North Atlantic, and toward East Asia during 1986–2010, leading to anomalous atmospheric circulation in East Asia and influencing the midsummer precipitation over NEC. The strengthening of the NPO and the enhanced relation between the NPO and North Atlantic Oscillation during 1986–2010 can explain the above changes. This study may deepen our understanding of the influence of NPO on the East Asian climate and may be meaningful for climate prediction.

Writing – original draft: Tingting Han
Writing – review & editing: Shengping He

1. Introduction

The North Pacific Oscillation (NPO), as an important intrinsic atmospheric variability, features a meridional seesaw pattern of SLP anomalies over the North Pacific (Rogers, 1981; Walker & Bliss, 1932; Wallace & Gutzler, 1981). The NPO is generally the second (first) principal mode of SLP during winter (summer) months, and a positive NPO phase is characterized by negative (positive) SLP anomalies centered around Alaska (near the Hawaiian Islands).

NPO variability has substantial influences on weather/climate conditions over North America, Australia, and the tropical Pacific (e.g., Chen & Wu, 2018; Linkin & Nigam, 2008; Park et al., 2020; Song et al., 2021; Sung et al., 2019; Vimont et al., 2001). Previous related studies have documented a close relation between the NPO and the East Asian climate (Guo & Sun, 2004; Li & Li, 2000; Wang et al., 2007). For example, Choi et al. (2011) claimed that a positive phase of the NPO during May could lead to intensified drought anomalies over North-east Asia during the following summer through modulation of northeasterly and descending motion anomalies. Analysis of observations and numerical simulations showed that a negative phase of the NPO during the previous winter is a contributor to prolonged spring-to-summer drought events over North China (Zhang et al., 2018). Tseng et al. (2020) documented that the southern lobe of the NPO is strongly connected with initiation of the East Asian winter monsoon in the region of the Philippine Sea. Moreover, the spring NPO could be a predictor of typhoon activity over the Northwest Pacific (Chen et al., 2015). Therefore, deepening our understanding of the influence of the NPO on the climate over eastern China is meaningful for the purpose of prevention and mitigation of related disasters.

Northeast China (NEC) is in the mid–high latitudes of Asia. Precipitation in NEC is highly concentrated during summer. Therefore, considerable efforts have been devoted to investigating the contributions of tropical and extra-tropical regimes to interannual and interdecadal variations in summer precipitation, such as the East Asian summer monsoon (Sun et al., 2017), sea surface temperature (SST) of in the tropical oceans (Han et al., 2017, 2020), cold vortex activity over NEC (Shen et al., 2011), Eurasian soil moisture content (Han et al., 2019; Zhu, 2011), and the Pacific Multidecadal Oscillation (Chen et al., 2019). Han et al. (2015) attributed interdecadal reduction in summer precipitation over NEC to the combination of the receded Northeast Asian summer monsoon and Arctic Sea ice anomalies after the late 1990s. Furthermore, Chen et al. (2020) noted that the Okhotsk High is responsible for interdecadal change in drought over NEC through modulation of the atmospheric circulation over Northeast Asia. Additionally, some studies have highlighted the effects of the preceding NPO on summer air temperature and precipitation anomalies over NEC. For example, Lian et al. (2013) claimed that the spring NPO is a potential precursor of summer air temperature in NEC. Zhou and Wang (2014) reported that the spring NPO acts as a link between wintertime ice in the Bering Sea and summer maize/rice yields across NEC. Therefore, the purpose of the present study was to explore the influence of the spring NPO on the following midsummer precipitation over NEC and to elucidate the possible mechanisms.

During recent decades, increasing attention has been paid to interdecadal changes in the relationship between the NPO and the East Asian climate. Specifically, Wang et al. (2007) identified that before the mid-1970s, stationary wave trains associated with the NPO propagated from the subtropical central Pacific to the North Pacific during winter, leading to an insignificant relation between the NPO and the East Asian climate. Subsequently, the NPO-related wave trains further propagated via a circumglobal route, leading to an enhanced connection between the NPO and the atmospheric circulation over East Asia. Furthermore, the relationship between the NPO and East Asian winter monsoon/precipitation has weakened since the late 1980s (Ao & Sun, 2016), owing to a decadal shift of the East Asian trough caused by decline of the East Asian winter monsoon (Park et al., 2014). Zhou and Xia (2012) suggested that a strong (weak) NPO was followed by decreased (increased) summer precipitation over the Huaihe River valley via modulation of the anomalous cyclone (anticyclone) over the western Pacific and descending (ascending) motion before the mid-1970s, and that this linkage was diluted thereafter. Recently, Hu et al. (2023) reported that the NPO is strongly linked to the occurrence of drought anomalies over southern China since the 2000s. They further attributed such intensification of the relation to the westward (southward) extension of the northern (southern) NPO lobe. However, the nonstationary variability in the connection between the NPO and midsummer precipitation over NEC, which is an important subject for climate prediction, remains unclear.

The remainder of this paper is organized as follows. Section 2 describes the data set and methods used in this study. Section 3 presents details of the changes in the relationship between the May NPO and the following

Table 1

Years Characterized by Positive and Negative NPO Indexes During the Two Periods of Strong and Weak NPO–Precip_NEC Relationship, Respectively

	The period of weak relation (1961–1985 and 2011–2020)		The period of strong relation (1986–2010)	
	Positive NPO	Negative NPO	Positive NPO	Negative NPO
Years	1961, 1969, 1973, 1974, 1976, 1979, 1980, 1983, 1985, 2011, 2015, 2017, 2018	1962, 1964, 1966, 1967, 1968, 1970, 1984, 2013, 2014	1988, 1990, 1991, 1993, 1994, 1995, 1998, 2005	1989, 1992, 1996, 1999, 2000, 2001, 2006, 2007, 2009, 2010
Total	13	9	8	10

midsummer precipitation over NEC and the possible mechanisms. Finally, a brief conclusion is presented in Section 4.

2. Materials and Methods

In this study, an advanced monthly precipitation observation data set (i.e., CN05.1) is used for 1961–2020 (Wu & Gao, 2013), on a $0.25^\circ \times 0.25^\circ$ latitude-longitude grid. This data set is constructed by interpolating data from more than 2400 meteorological stations in China. The monthly atmospheric reanalysis data set is extracted from the National Center for Environment Prediction and National Center for Atmospheric Research for 1948–2020, with a horizontal resolution of $2.5^\circ \times 2.5^\circ$ (Kalnay et al., 1996). Variables used in the present study include sea level pressure, horizontal wind (UV), geopotential height (Z), specific humidity, and vertical motion. The North Atlantic Oscillation (NAO) index is derived from the Climate Prediction Center: <https://www.cpc.ncep.noaa.gov/products/precip/CWlink/pna/nao.shtml>.

The common time period for this study spans from 1961 to 2020. NEC is defined as the region north of 38°N and east of 115°E within China. Midsummer precipitation refers to the summation of precipitation amounts during July and August. A precipitation index (Precip_NEC) is defined as the normalized area-weighted average of summer precipitation over NEC. The empirical orthogonal function (EOF) analysis was performed on SLP during May over the North Pacific ($10^\circ\text{--}70^\circ\text{N}$, $140^\circ\text{E--}120^\circ\text{W}$; Figure S1 in Supporting Information S1). The first and second EOF modes explain 33.3% and 19.1% of total variance, respectively. The NPO index is defined as the time series corresponding to the leading EOF1 mode of SLP, which exhibits a north-south dipole pattern over the Pacific sector. Positive (negative) NPO/NAO years are selected as years characterized by values greater (less) than 0.5 (-0.5) (Tables 1 and 2).

Composite, regression and correlation analyses are performed to investigate the atmospheric circulation anomalies associated with the Precip_NEC and NPO. The student's *t*-test is used to determine statistical significance. Additionally, linear trends have been eliminated from all fields before analysis to isolate the interannual variation.

3. Results

3.1. Interdecadal Changes in the Linkage Between the May NPO and Summer Precipitation in NEC

A significant positive relationship was observed to exist between the NPO in May and precipitation in NEC (Precip_NEC) during summer, with a correlation coefficient of 0.27 during 1961–2020 (above the 95% confidence level), as implied by previous works on the influence of the spring NPO on summer precipitation over China

Table 2

Years Characterized by Positive and Negative NAO Indexes During the Periods of Strong and Weak NPO–Precip_NEC Relationship, Respectively

	The period of weak relation (1961–1985 and 2011–2020)		The period of strong relation (1986–2010)	
	Positive NAO	Negative NAO	Positive NAO	Negative NAO
Years	1963, 1970, 1972, 1976, 1978, 1984, 2013, 2018	1965, 1967, 1968, 1977, 1979, 1980, 2012, 2014, 2017, 2019	1986, 1987, 1988, 1989, 1992, 1999, 2000, 2007, 2009	1990, 1993, 1995, 1996, 1998, 2005, 2006, 2008, 2010
Total	8	10	9	9

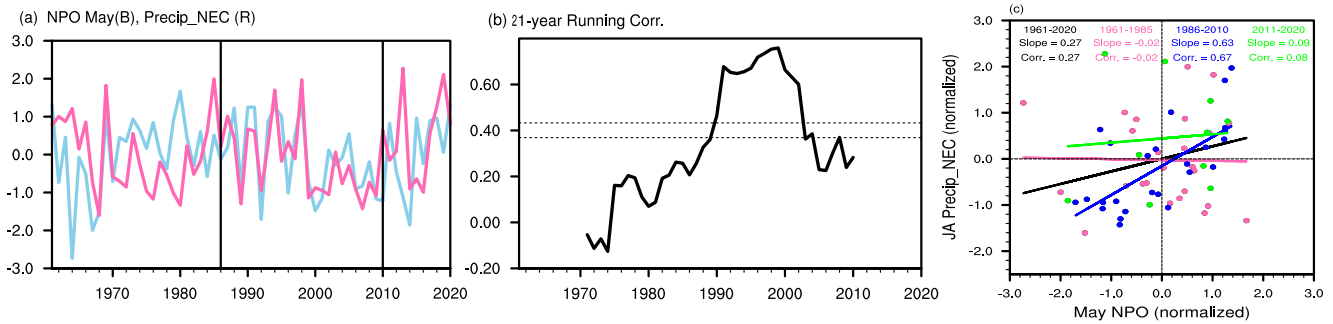


Figure 1. (a) Temporal evolutions of the May NPO index (blue line) and the midsummer precipitation index at Northeast China (red line), both of which have been normalized and detrended. The precipitation index (Precip_NEC) is defined as the normalized area-weighted average of summer precipitation at Northeast China. The NPO index is defined as the time series corresponding to the leading EOF mode of SLP over the North Pacific during May. (b) The 21-year sliding correlation coefficients between NPO and Precip_NEC indices. Horizontal broken lines denote 95% and 90% confidence level, based on Student's *t*-test. (c) Scatter plot of Precip_NEC against the NPO indices during four periods: 1961–2020 (black), 1961–1985 (red), 1986–2010 (blue), and 2011–2020 (green).

(e.g., Choi et al., 2011; Zhou & Xia, 2012). To detect whether instability exists in that relationship, Figure 1a presents the temporal evolutions of both indexes. Notably, the linkage between the NPO and Precip_NEC indexes varies with time, and in-phase variations are observed during the period from the mid-1980s to the 2010s, together with weak connection of the NPO to the following summer precipitation in NEC before the mid-1980s and during the 2020s. Figure 1b depicts the 21-year running correlation coefficients between the two indices. Insignificant negative correlation coefficients are observed before the mid-1970s. The correlations turn to be positive afterward and become significant after the 1990s, which have weakened since the mid-2000s. When the sliding window width changes to 17, 19, and 23 years, this unstable relation is also apparent (figures not shown). To confirm the interdecadal shifts in the interannual relationship between the NPO and Precip_NEC, two subperiods were selected as the period of the significant relationship (i.e., 1986–2010; hereafter, Sig. period) and the period of the insignificant relationship (i.e., 1961–1985 and 2011–2020; hereafter, Insig. period). The correlation coefficients between the NPO and Precip_NEC indexes, as depicted in Figure 1c, are weak for 1961–1985 (−0.02) and 2011–2020 (0.08). By comparison, the NPO index covaries consistently with the Precip_NEC index during the Sig. period (correlation coefficient: 0.67, above the 99% confidence level).

The respective spatial distributions of summer precipitation anomalies over NEC between positive and negative NPO index years during the Insig. and Sig. periods are illustrated in Figures 2a and 2b. During the Insig. period, the precipitation anomalies associated with the positive NPO phase are barely significant over NEC, excluding a small part in the west. However, for the Sig. period, a positive NPO index during May is followed by distinct positive precipitation anomalies over most of NEC. Consistent results can be obtained based on the precipitation data set from the Global Precipitation Climatology Center (GPCC; figures omitted). Additionally, the SLP anomalies during the preceding May between the positive and negative Precip_NEC index years for the two periods are shown in Figures 2c and 2d. During the Insig. period, the positive precipitation anomalies over NEC are led by weak SLP anomalies over the North Pacific (Figure 2c). For the Sig. period, more precipitation over NEC follows a dipole pattern of abnormal SLP with a negative center to the north of the Aleutian Islands and a positive center at around 30°N to the east of the dateline, which resembles a classical positive phase of the NPO (Wallace & Gutzler, 1981; Figure 2d). These results imply that the influence of the May NPO on the following summer precipitation in NEC is unstable, being pronounced during 1986–2010 but insignificant before the mid-1980s and during the 2020s. El Niño–Southern Oscillation (ENSO) has been regarded as one of the strongest internal variabilities that has significant impacts on interannual climate variabilities. However, the ENSO has little influences on the decadal shifts of the relationship between the May NPO and the following midsummer precipitation in NEC (Figure S2 in Supporting Information S1).

To further explore the changes in the relationship during the past six decades, the atmospheric circulation anomalies associated with the NPO were examined. During the Sig. period, a positive NPO index during May is followed by a meridional dipole pattern of horizontal wind anomalies over the region from East Asia to the western Pacific, together with an anomalous anticyclone centered over the subtropical western Pacific and a cyclone stretching from the Northwest Pacific to NEC (Figure 3b). A southwesterly flow at the western flank of the anticyclone prevails over eastern China, facilitating the transport of moisture northward to NEC. The easterly

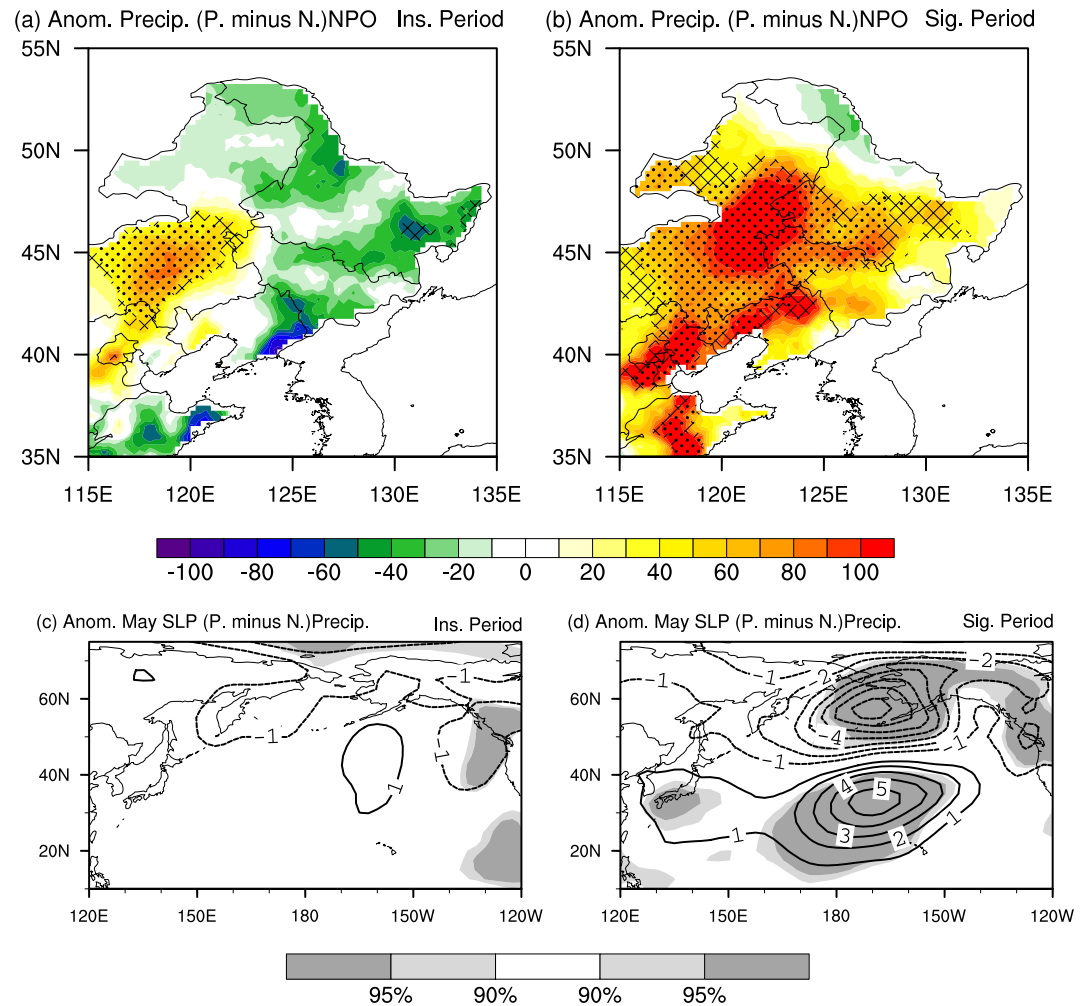


Figure 2. Differences in summer precipitation anomalies (mm) between positive and negative NPO years during the periods of (a) insignificant and (b) significant NPO–Precip_NEC relationship. Stippled (crossed) areas indicate values that significantly exceed the 95% (90%) confidence level, estimated using the Student's *t*-test. Differences in SLP anomalies (mb) during May between more and less summer precipitation years during the periods of (c) insignificant and (d) significant NPO–Precip_NEC relationship. Dark (light) shading indicates values that significantly exceed the 95% (90%) confidence level, estimated using the Student's *t*-test.

anomalies at the northern flank of the cyclone elongate from the North Pacific westward to northern NEC. Correspondingly, a positive NPO index is characterized by profound moisture divergence anomalies over the subtropical western Pacific and the South China Sea. The dominance of anomalous southwesterly or southeasterly flows over eastern China conveys water vapor northward to NEC across the southern boundary (Figure 3d). Additionally, anomalous moisture divergence emerges over the North Pacific, together with anomalous easterly currents carrying moisture from the northern Pacific westward to NEC across the eastern boundary. Therefore, anomalous moisture convergence dominates NEC, which provides sufficient moisture for summer precipitation. By contrast, during the Insig. period, the positive NPO phase is associated with a zonal dipole mode of horizontal wind anomalies during summer, with an anomalous cyclone centered over the high latitudes of the Northwest Pacific and an anticyclone centered over the Northeast Pacific (Figure 3a). The wind fields over East Asia and over the subtropical Northwest Pacific are both insignificant. Accordingly, the moisture transport anomalies are weak over eastern China and NEC (Figure 3c), leading to a weak NPO–Precip_NEC relation (Figures 2a and 2c).

Convective motion is essential for precipitation processes. Figure 4 illustrates the divergence and vertical movement anomalies related to the NPO. For the Sig. period, a positive NPO index is featured with remarkable convergence (divergence) anomalies in the lower (upper) troposphere over NEC, which further excite prominent local

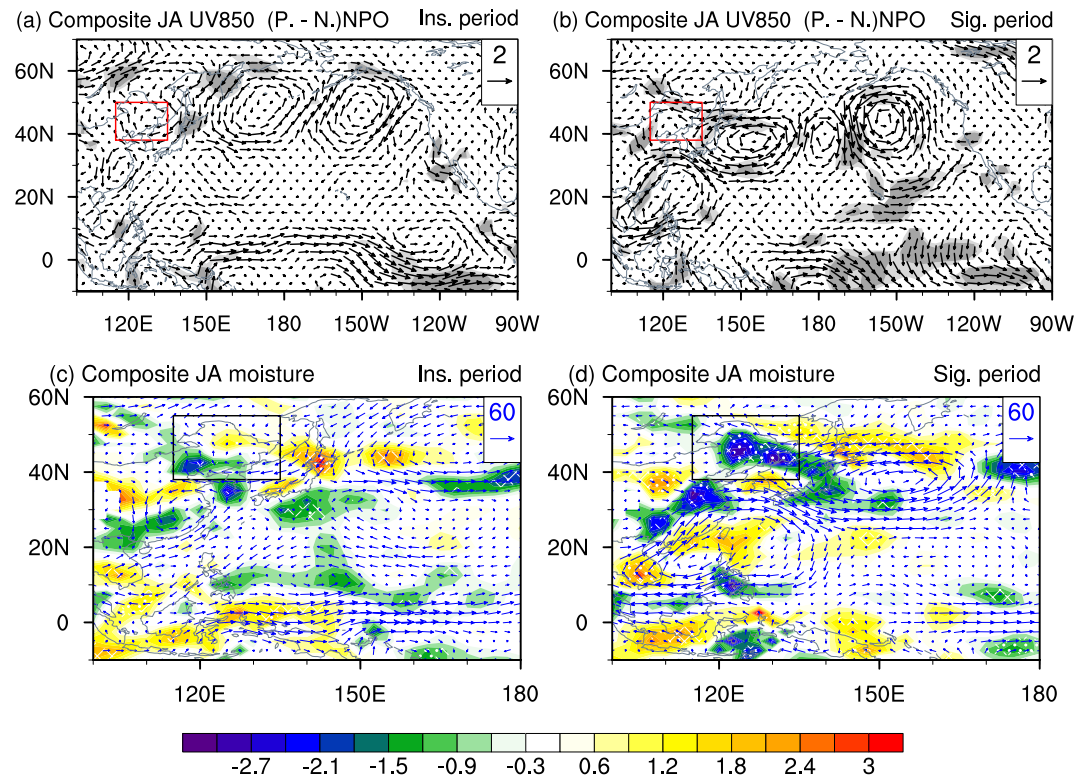


Figure 3. Differences in summer (a, b) horizontal wind fields at 850 hPa (m/s) and (c, d) vertically integrated moisture flux (vectors, $\text{kg}/(\text{m} \times \text{s})$) and divergence (shading, $10^{-6} \text{ kg}/(\text{m}^2 \times \text{s})$) between positive and negative NPO years during the periods of (left) insignificant and (right) significant NPO–Precip_{NEC} relationship. Dark (light) shading in (a, b) indicates values that significantly exceed the 95% (90%) confidence level, estimated using the Student's *t*-test. Stippled (crossed) areas in (c, d) indicate the moisture divergence anomalies that significantly exceed the 95% (90%) confidence level, estimated using the Student's *t*-test.

ascending motion (Figures 4b, 4d, and 4f). In contrast, during the Insig. period, the NPO-related divergent circulation anomalies are weak over NEC in both the lower and the upper layers, accompanied by weak vertical motion anomalies (Figures 4a, 4c, and 4e). The above results indicate that the strengthened influence of the May NPO on the following summer atmospheric circulation over East Asia (such as horizontal wind, moisture transport, and vertical movement) contributed to intensification of the NPO–Precip_{NEC} relation during the period from the mid-1980s to the 2010s.

3.2. Changes of Rossby Wave Trains in Association With the May NPO

The above results prompt interest in the reasons for the interdecadal change in the effects of the May NPO on atmospheric circulations over East Asia during the following summer. Subseasonal evolutions of the upper-level horizontal wind anomalies from May to midsummer associated with the May NPO index during both periods are illustrated in Figure 5. A positive phase of the May NPO is associated with a meridional dipole of atmospheric circulation anomalies over the North Pacific, together with cyclonic wind fields over the Aleutians Islands and anticyclonic wind anomalies over mid-latitude regions of the North Pacific (Figures 5a and 5b). Comparatively, the NPO-related circulation anomalies are more intensified over the region from North America to the North Atlantic during the Sig. period than during the Insig. period. Specifically, the positive NPO index is accompanied by notable anticyclonic wind anomalies over northwestern North America and the northern North Atlantic, and by cyclonic wind anomalies over southwestern and eastern parts of North America and over the southern North Atlantic during the Sig. period, which cannot be observed during the Insig. period. In the following June, alternation of anomalous anticyclones and cyclones related to the May NPO dominates the mid-latitudes and extends from the Northeast Pacific eastward to North America and the North Atlantic, exhibiting a wave-like pattern (Figure 5d). During the subsequent summer, such a wave-like pattern of wind anomalies propagates eastward over

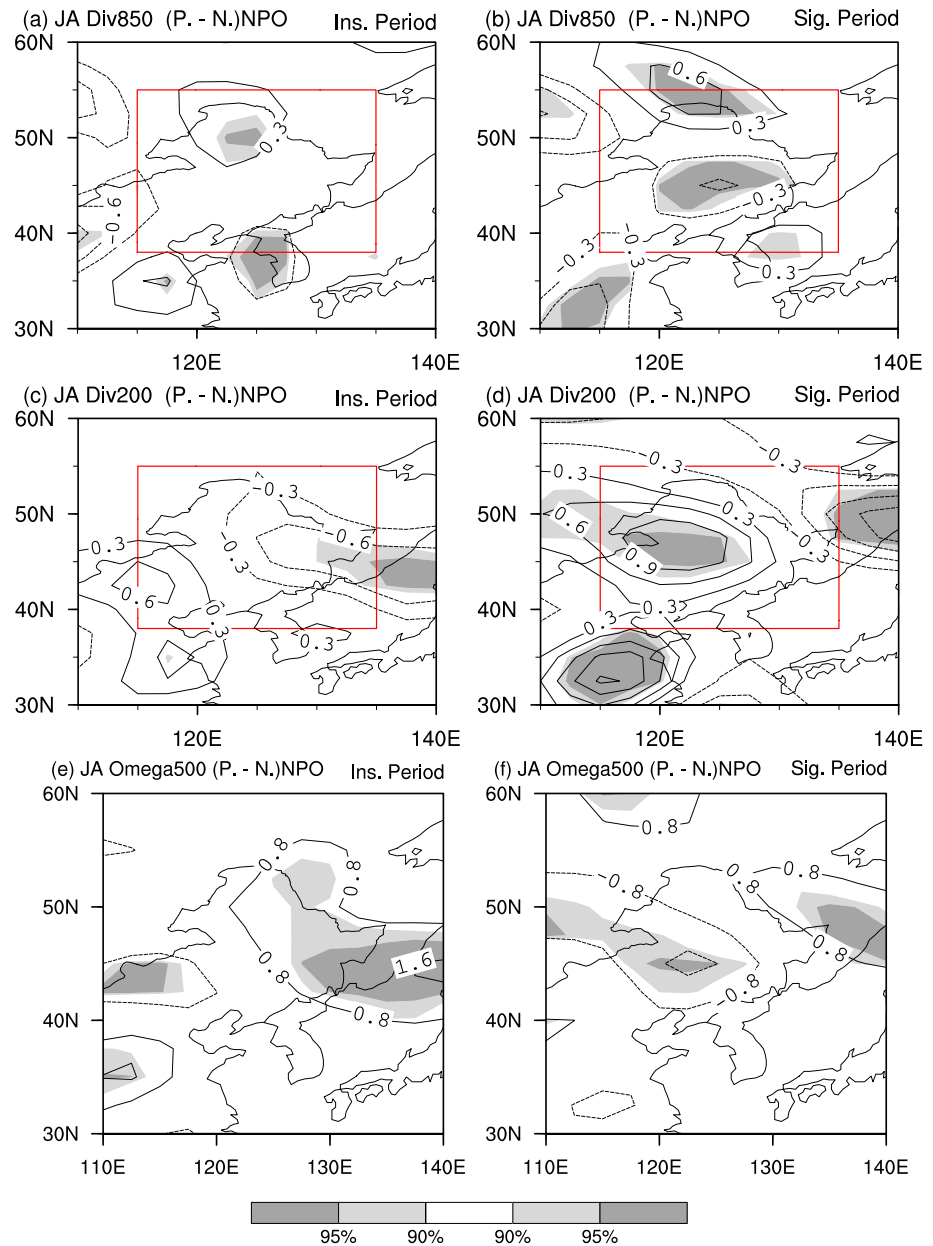


Figure 4. Same as Figures 3a and 3b, but for (a, b) 850-hPa horizontal wind divergence anomalies ($10^{-6}/s$), and (c, d) 200-hPa horizontal wind divergence anomalies ($10^{-6}/s$) and (e, f) 500-hPa vertical movement anomalies (10^{-2} Pa/s).

the mid-latitude region of Eurasia (Figure 5f) whereby the NPO has a lagged influence both on the atmospheric circulation over East Asia and on NEC precipitation. To a lesser extent, the NPO-related wind anomalies display a wave-like pattern extending from the North Pacific to the North Atlantic and on to Northeast Asia through a polar route in June during the Insig. period (Figure 5c), which weakens during the following summer (Figure 5e).

Wang et al. (2007) suggested that the enhanced relation between the NPO and the East Asian winter monsoon is related to strong stationary wave activities over Eurasia. We speculated that the May NPO could induce an eastward-propagating stationary Rossby wave train during the period of significant NPO–Precip_NEC relation, which fails during the period of insignificant NPO–Precip_NEC relation. This can be observed in Figure 6, which depicts the subseasonal variations in the linear regression of the 300-hPa quasigeostrophic streamfunction and the related wave activity flux with regard to the May NPO index. Wave activity flux, which is calculated based on Plumb's formulation (Plumb, 1985), is a robust indicator of the propagation of stationary Rossby

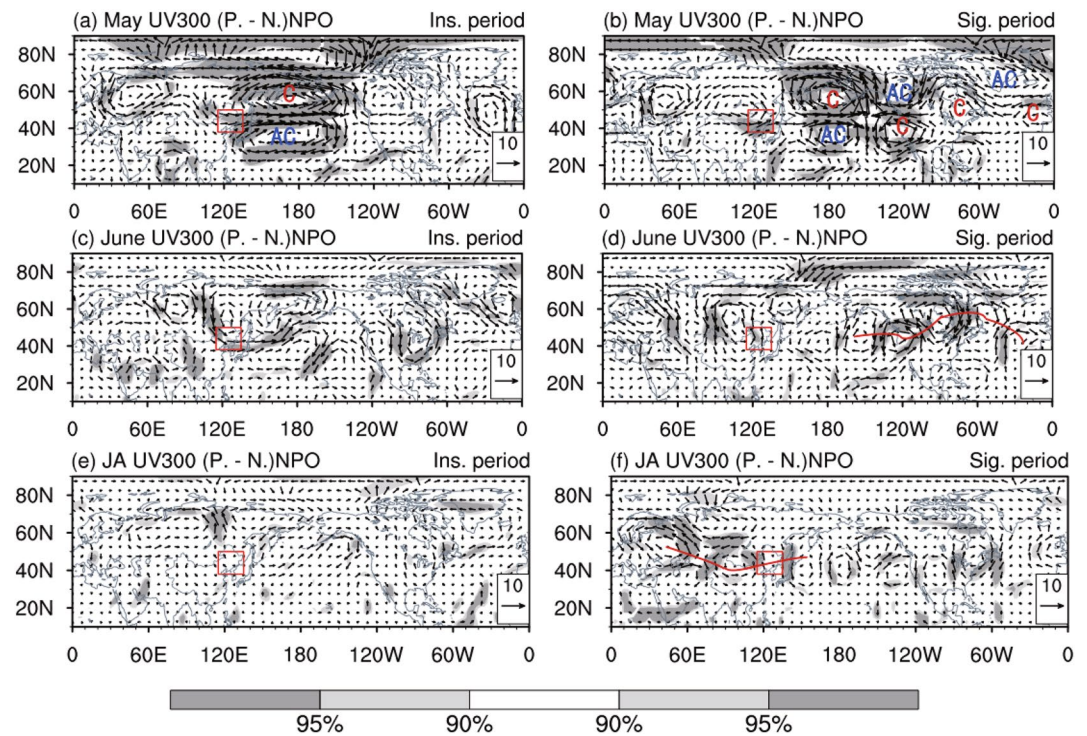


Figure 5. Differences in 300-hPa horizontal wind anomalies (m/s) between positive and negative NPO years during the periods of (left) insignificant and (right) significant NPO–Precip_NEC relationship: (a, b) May, (c, d) June, and (e, f) midsummer. Dark (light) shading indicates values that significantly exceed the 95% (90%) confidence level, estimated using the Student's *t*-test.

waves. Associated with a positive phase of the NPO, clear eastward propagation of anomalous Rossby waves in the upper troposphere is visible over the mid-latitudes of the Western Hemisphere during the Sig. period (Figure 6b). Having originated over the North Pacific, the wave train then bifurcates into two branches, with one propagating eastward over the high latitudes of North America and the North Atlantic along a polar path, and the other diffusing southeastward toward the subtropical North America. These two wave trains can also be recognized in the streamfunction anomalies associated with the NPO. The alternative appearance of significant negative–positive–negative–positive streamfunction anomalies exhibits a wave-like pattern, extending from the North Pacific eastward to the North Atlantic (Figure 6b). Previous studies have revealed that the advection of vorticity by the divergent component of the flows could excite Rossby waves (Sardeshmukh & Hoskins, 1988). As shown in Figure 7b, the NPO is coincident with anomalous divergence over the Northeast Pacific, consistent with the location of the source of the Rossby wave anomalies; hence, the Rossby wave trains are driven over the downstream region. Subsequently, during June, the NPO-related divergent wind anomalies and source of the Rossby waves extend eastward and become larger in magnitude over eastern North America (Figure 7d). Accordingly, a set of wave trains extends from North America to Eurasia (Figure 6d). During the following summer, the Rossby wave source shifts eastward and strengthens over the North Atlantic, and a conspicuous Rossby wave-train pattern extends from the North Atlantic eastward to NEC (Figures 6f and 7f). Accordingly, alternating cyclonic and anticyclonic anomalies expand over the mid-latitudes of Eurasia (Figure 5f). The Rossby wave trains driven by the NPO, which propagate from the North Pacific eastward to North America, the North Atlantic, and then on to East Asia on the subseasonal time scale during summer months, provide an evidence of the lagged impact of the May NPO on the following summer atmospheric circulation and moisture transport over East Asia and NEC precipitation.

In contrast, during the Insig. period, the May NPO is concurrent with anomalous divergence anomalies and the source of Rossby waves over the North Pacific, which are quantitatively weaker than those during the Sig. period (Figures 7a and 7b). Consequently, the wave trains associated with the NPO, which propagate from the North Pacific to northern North America, are weaker over the North Atlantic (Figure 6a). During the following June and

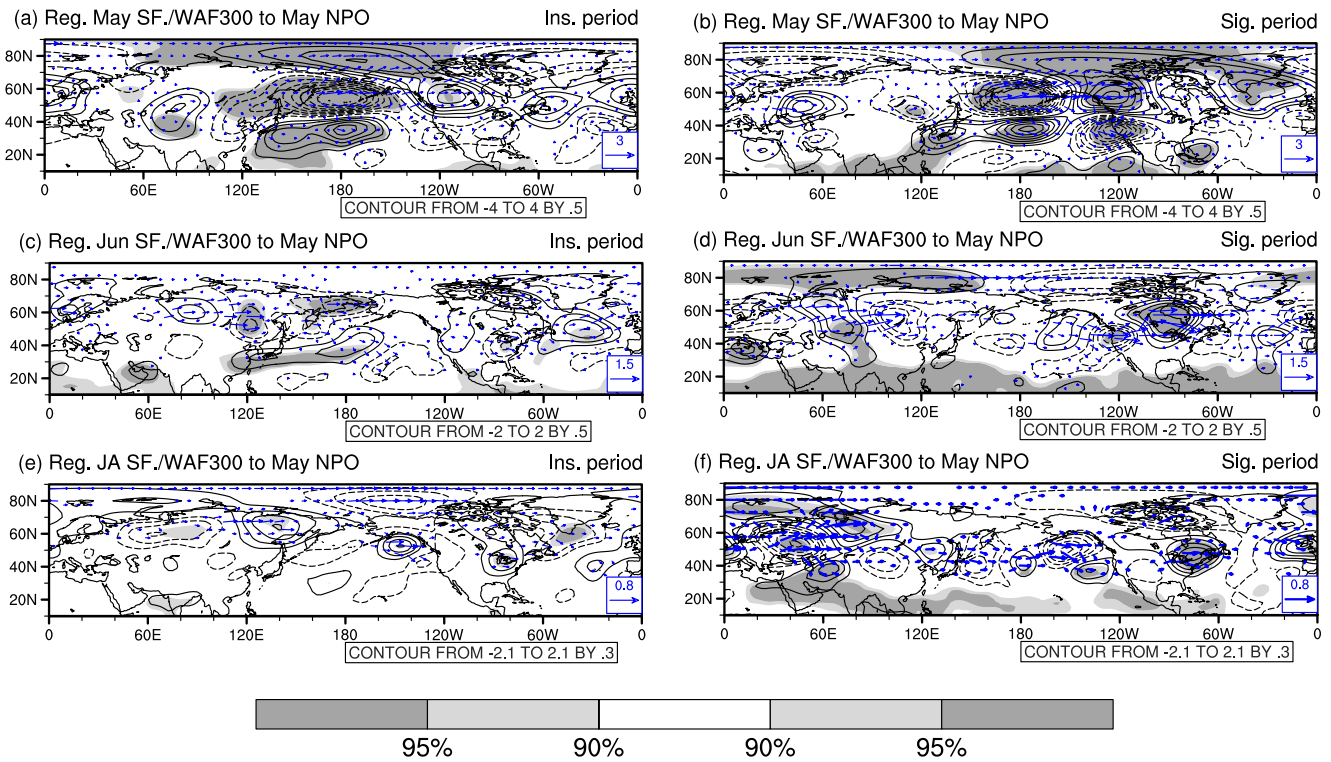


Figure 6. Streamfunction (contours, $10^6 \text{ m}^2/\text{s}$) and wave activity flux (vectors, m^2/s^2) anomalies at 300 hPa regressed against the May NPO index during the periods of (left) insignificant and (right) significant NPO–Precip_NEC relationship: (a, b) May, (c, d) June, and (e, f) midsummer. Dark (light) shading indicates streamfunction anomalies that significantly exceed the 95% (90%) confidence level, estimated using the Student's *t*-test. Vectors with magnitude of <0.1 are not plotted.

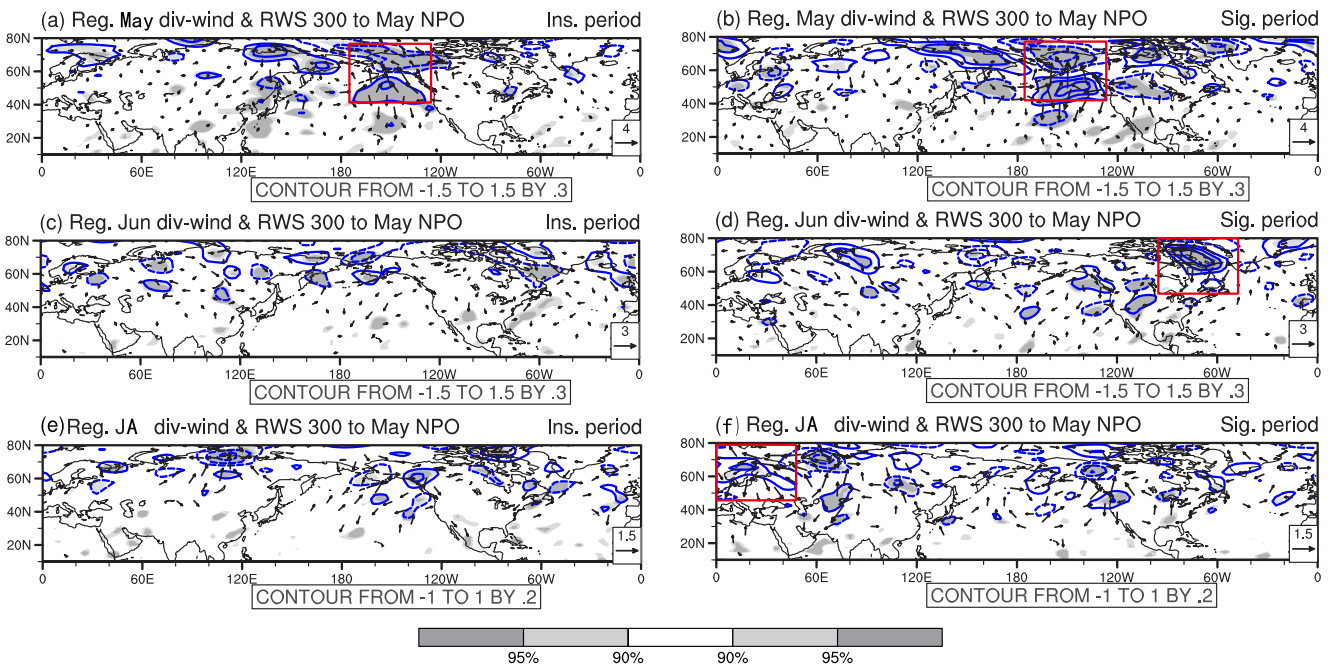


Figure 7. Rossby wave source ($10^{-9}/\text{s}^2$) and divergent wind component (m/s) anomalies at 300 hPa regressed against the May NPO index during the periods of (left) insignificant and (right) significant NPO–Precip_NEC relationship: (a, b) May, (c, d) June, and (e, f) midsummer. Dark (light) shading indicates Rossby wave source anomalies that significantly exceed the 95% (90%) confidence level, estimated using the Student's *t*-test. Vectors with magnitude of <0.5 are not plotted.

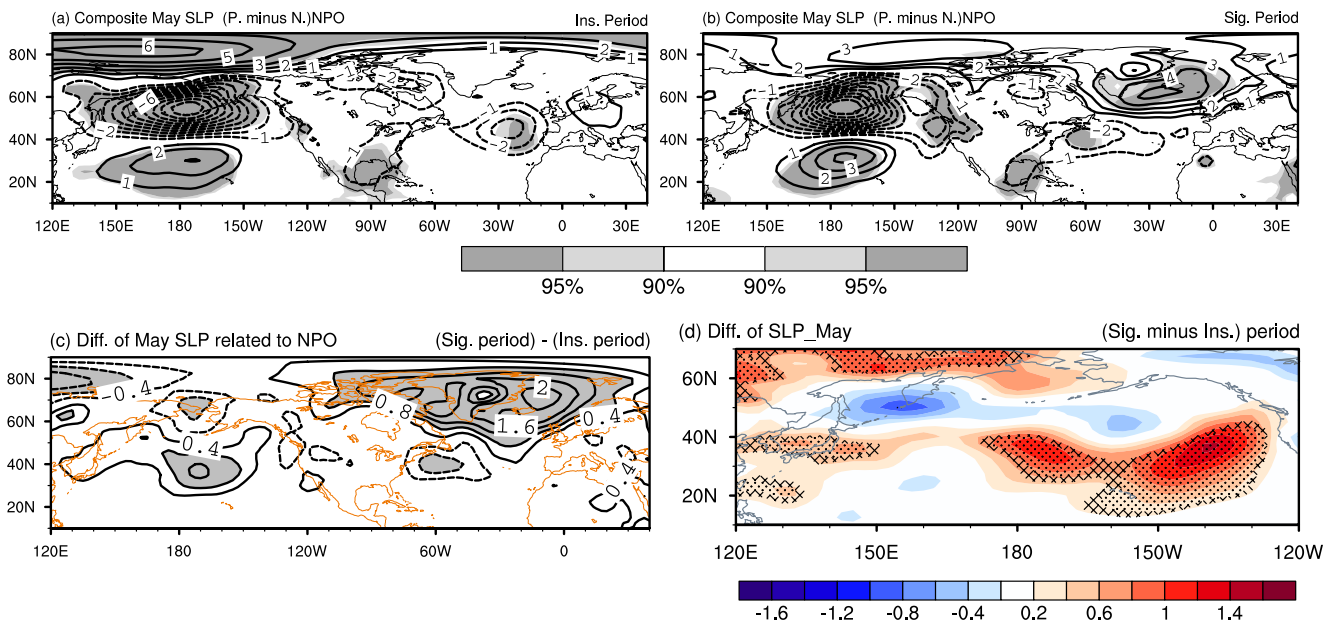


Figure 8. Differences in May SLP anomalies between positive and negative NPO years during the periods of (a) insignificant and (b) significant NPO–Precip_NEC relationship. Dark (light) shading indicates values that significantly exceed the 95% (90%) confidence level, estimated using the Student's *t*-test. (c) Changes in SLP anomalies between the two periods, that is, (b) minus (a). Values with magnitude of >0.8 mb are shaded. (d) Differences in standard deviation of SLP (mb) over the North Pacific between the two periods. Stippled (crossed) areas indicate values that significantly exceed the 95% (90%) confidence level, estimated using the Student's *t*-test.

midsummer, anomalous divergence and the source of Rossby waves vanish over North America and the North Atlantic, respectively (Figures 7c and 7e). As expected, the Rossby wave trains recede during summer (Figures 6c and 6e). Hence, the May NPO has an insignificant influence on the following summer circulation anomalies over East Asia and on NEC precipitation.

It is speculated that the strengthened NPO might contribute to intensification of the Rossby wave trains associated with the NPO. Composite results of SLP between positive and negative NPO years during the Insig. period and Sig. period are shown in Figures 8a and 8b, respectively. By comparison, the SLP anomalies associated with the NPO are quantitatively larger and spatially broader over the North Pacific during the Sig. period than during the Insig. period. Additionally, strengthening of the NPO can be seen from the differences of the SLP anomalies between two periods, together with enhancement in the northern and southern lobes of the May NPO and eastward expansion of the northern lobe to North America during the Sig. period (Figure 8c). The interdecadal change in the leading mode of SLP (i.e., the NPO pattern) may contribute to the interdecadal shifts in the interannual relationship between the May NPO and the mid-summer precipitation in NEC. Moreover, the interannual variability in SLP over the North Pacific becomes greater during the Sig. period (Figure 8d), which might contribute to the larger amplitude of the NPO and further induce intensified NPO-related Rossby wave anomalies. The interannual variability of the SST intensifies at the midlatitude North Pacific during the Sig. period, which is not discussed in this study due to the release of turbulent heat flux from atmosphere to ocean in situ (figures not shown).

3.3. Strengthened Relation Between the NPO and the NAO

Notably, the NPO co-occurs with distinct SLP anomalies over the North Atlantic during May in the Sig. period (Figure 8b). To be specific, the positive NPO phase is concurrent with the prevalence of positive SLP anomalies over the high latitudes of the North Atlantic and negative values to the south, that is, a negative NAO phase, which cannot be observed during the Insig. period (Figure 8a). This result implies strengthening of the out-of-phase relation between the NPO and NAO during the Sig. period, which might be related to change in the background circulation. EOF analysis was conducted on the SLP during May over the region extending from the North Pacific to the North Atlantic (20°–70°N, 120°–360°E) during the two periods (Figure 9). For the Insig. period, the first

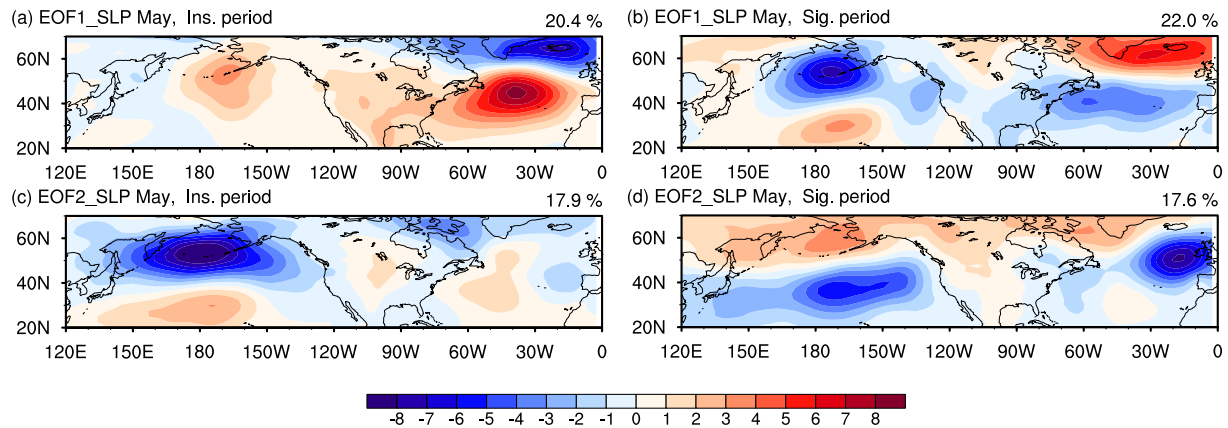


Figure 9. The first and second empirical orthogonal function (EOF) modes of SLP over the region stretching from the North Pacific to the North Atlantic (20°–70°N, 120°–360°E) during the periods of (a, c) insignificant and (b, d) significant NPO–Precip_NEC relationship.

EOF mode features a meridional dipole pattern of SLP anomalies over the North Atlantic, together with relatively weak signals centered over the Aleutian Islands, that is, the EOF1 mode indicates coexistence of the positive NAO phase and a weakened Aleutian Low (Figure 9a). Moreover, the second EOF mode is characterized by a meridional dipole pattern of SLP anomalies over the North Pacific (i.e., a positive NPO phase), together with weak anomalies over the North Atlantic (Figure 9c). It implies that the NPO and NAO are independent of each other during the Insig. period. Such a weak relation is confirmed by the composites of SLP anomalies between positive and negative NAO/NPO years during the Insig. period (Figures 8a and 10a). The positive NAO phase is concomitant with negative and positive SLP anomalies over high- and mid-latitude regions of the North Atlantic, respectively, together with weak anomalies over the North Pacific (Figure 10a). Additionally, the correlation coefficients between the NPO and NAO indexes are insignificant, with values of 0.02 and 0.17 during 1961–1985 and 2011–2020, respectively (Figure 11a). The preceding May NAO has a minimal impact on summer precipitation over NEC, with correlation coefficients of 0.29 and 0.04 during 1961–1985 and 2011–2020, respectively (Figure 11b).

During the Sig. period, the leading EOF mode is characterized by a positive NPO mode over the North Pacific and a negative NAO mode over the North Atlantic (Figure 9b). Consistently, the composite of SLP anomalies between positive and negative NAO years features negative and positive anomalies over the high- and mid-latitude regions of the North Atlantic, respectively, coinciding with positive values centered over the Aleutian Islands and negative anomalies centered over the Hawaiian Islands (i.e., the negative NPO phase; Figure 10b). Prominent correlation exists between the NPO and NAO indexes, with a value of -0.50 (above the 95% confidence level) during 1986–2010 (Figure 11a). Additionally, the effects of the preceding May NAO on summer precipitation in NEC become intensified, with a correlation coefficient of -0.44 (above the 95% confidence level; Figure 11b).

The strengthened connection between the NPO and the NAO might further contribute to the intensified effects of the May NPO on the Rossby wave trains over the mid-latitudes during subsequent summer months. When

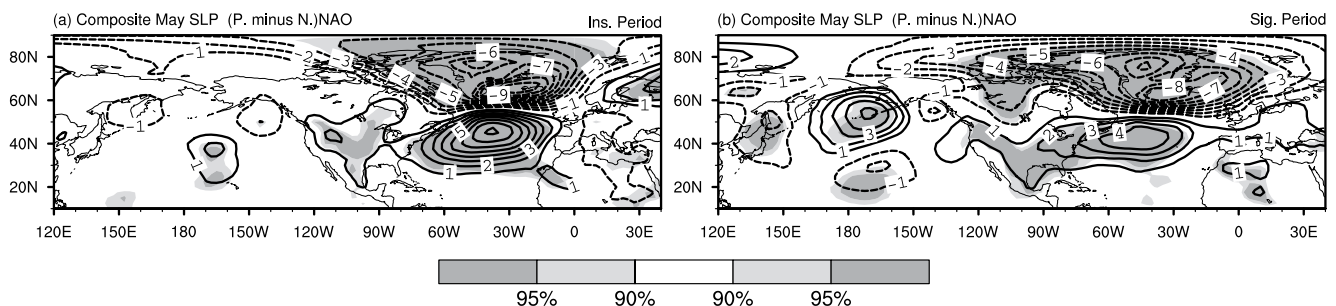


Figure 10. Differences in SLP anomalies (mb) during May between positive and negative NAO years during the periods of (a) insignificant and (b) significant NPO–Precip_NEC relationship. Dark (light) shading indicates values that significantly exceed the 95% (90%) confidence level, estimated using the Student's *t*-test.

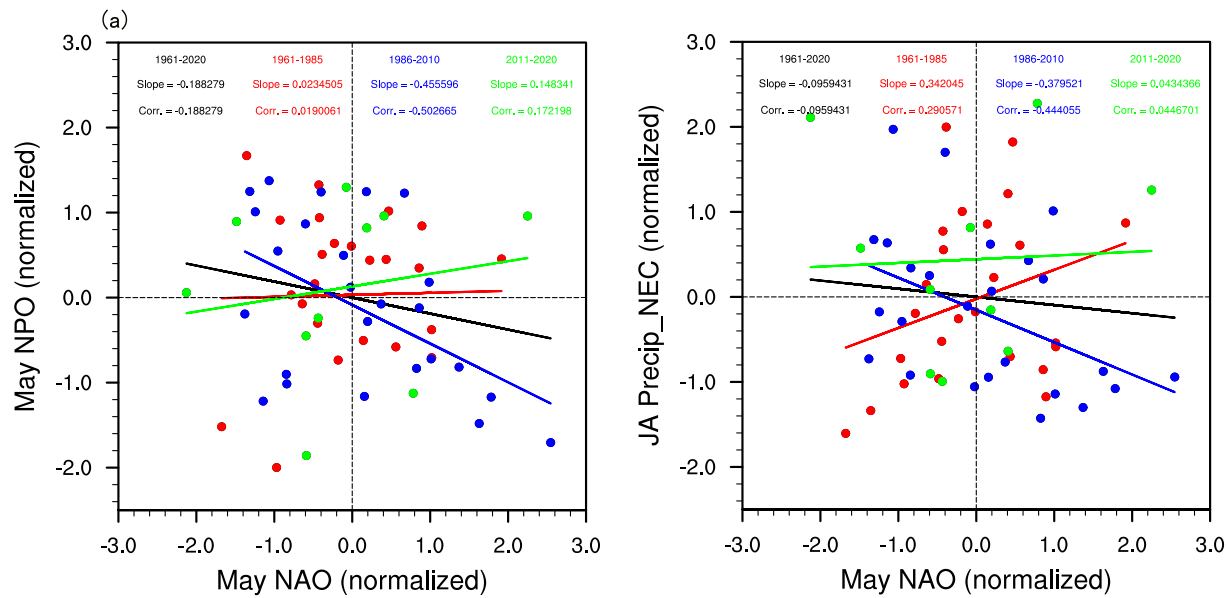


Figure 11. (a) Scatter plot of May NPO against NAO indices during four periods: 1961–2020 (black), 1961–1985 (red), 1986–2010 (blue), and 2011–2020 (green). (b) Scatter plot of Precip_NEC against the NAO indices during four periods: 1961–2020 (black), 1961–1985 (red), 1986–2010 (blue), and 2011–2020 (green).

a positive NPO phase coincides with a negative NAO phase during May, there is an obvious zonally oriented teleconnection wave train, which mainly initiates from the North Pacific and crosses North America to the North Atlantic (Figure 12a). Apparent Rossby wave source anomalies are evident over the North Pacific (Figure 13a). The teleconnection wave trains propagate continuously from North America eastward to the North Atlantic and further on over the Eurasian continent during June (Figure 12b). In the subsequent midsummer, the anomalous wave trains are enhanced and propagate eastward over the region extending from the North Atlantic toward East Asia in mid-latitude regions, triggered by an anomalous Rossby source over the North Atlantic (Figures 12c and 13c). The eastward shifts of the source of the Rossby waves and the eastward propagation of the teleconnection wave trains on the subseasonal time scale are consistent with those features in association with the NPO during the Sig. period (Figures 6 and 7).

Previous studies have determined that the NAO exerts considerable impacts on the atmospheric circulation over East Asia through the Rossby wave pattern (Han et al., 2018; Sun et al., 2008). The previous May NAO is followed by dominance of the anomalous Rossby wave source over the North Atlantic during summer (Figure 14a), which is stimulated by advection of divergence anomalies (Sardeshmukh & Hoskins, 1988). Consequently, the circumglobal teleconnection wave train derives from the North Atlantic and propagates eastward to NEC over mid-latitude Eurasia (Figure 14b). The above result suggests that a strengthened relationship between the NPO and the NAO is partially responsible for the eastward propagation of NPO-related Rossby wave trains in mid-latitude regions on the subseasonal time scale.

4. Conclusions

This study investigated the temporal variations in the connection between the May NPO and midsummer precipitation in NEC during the past six decades. The May NPO had a pronounced positive influence on the following midsummer precipitation over NEC during 1986–2010 (i.e., the Sig. period), whereas the relationship was statistically insignificant during 1961–1985 and 2011–2020 (i.e., the Insig. period).

Further results indicated that the magnitude of the May NPO was stronger during the Sig. period than during the Insig. period. The strengthened NPO triggered intensified Rossby wave source anomalies over the North Pacific in May during the Sig. period. This was accompanied by a zonally oriented teleconnection wave train over the mid-latitudes of the Western Hemisphere, which originated over the North Pacific and crossed North America to reach the North Atlantic. During the subsequent June and midsummer, the Rossby wave source shifted eastward to eastern North America and the North Atlantic, respectively. Simultaneously, a set of teleconnection

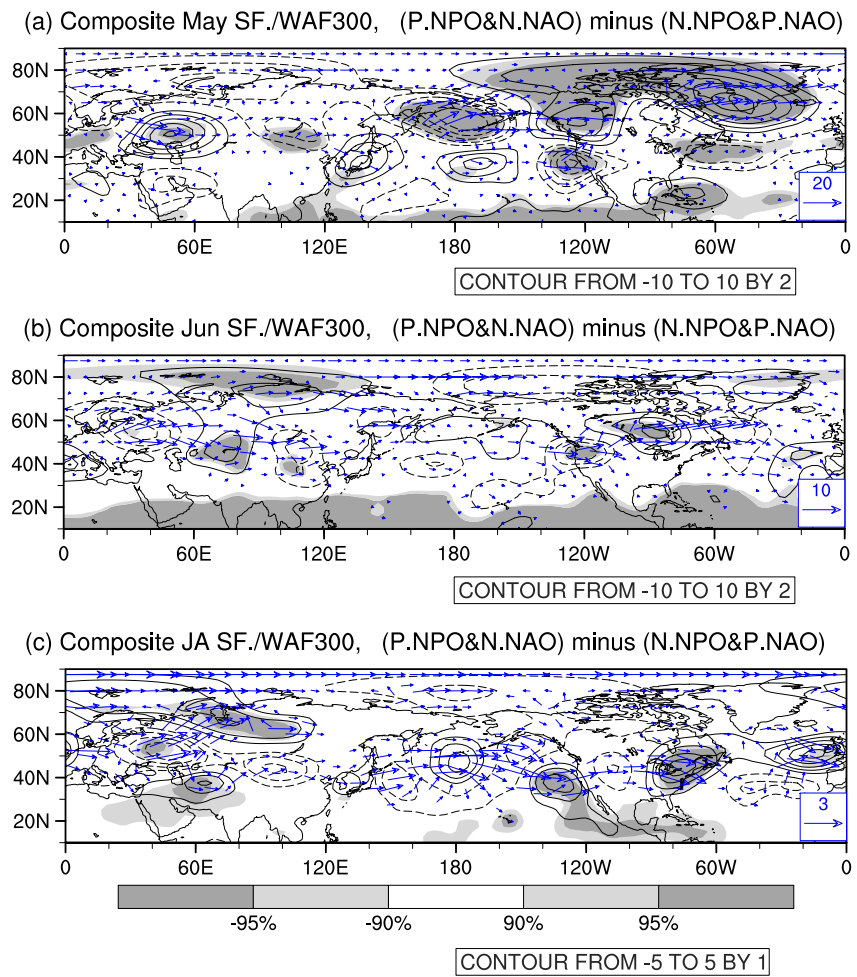


Figure 12. Differences in 300-hPa streamfunction (contours, $10^6 \text{ m}^2/\text{s}$) and wave activity flux anomalies (vectors, m^2/s^2) during midsummer between the NPO+/NAO- and NPO-/NAO+ years during the period of significant NPO–Precip_{NEC} relationship: (a, b) May, (c, d) June, and (e, f) midsummer. Dark (light) shading indicates streamfunction anomalies that significantly exceed the 95% (90%) confidence level, estimated using the Student's *t*-test. Vectors with magnitude of <0.5 are not plotted.

wave trains propagated continuously eastward from North America, across the North Atlantic, and further on to NEC. Therefore, the positive NPO phase was followed by an anomalous anticyclone and an anomalous cyclone over the subtropical western Pacific and the Northwest Pacific, respectively. Southerly anomalies across the southern boundary and easterly anomalies across the eastern boundary of NEC resulted in prominent local moisture convergence anomalies. Additionally, the lower-level convergence and upper-level divergence anomalies associated with the positive NPO phase excited local ascending motion over NEC. Sufficient moisture content and enhanced convection jointly contributed to increased midsummer precipitation over NEC. Furthermore, a strengthened NPO might be attributable to intensification in the standard deviation of SLP over the North Pacific.

Notably, the background circulation changed over the North Pacific–North Atlantic region during the two periods. During the Insig. period, the NPO and NAO were mutually independent, whereas during the Sig. period, the positive (negative) NPO coincided with the negative (positive) NAO. An enhanced out-of-phase connection between the NPO and the NAO is considered partially responsible for the intensified Rossby wave trains related to the NPO because the NAO could lead to eastward propagation of Rossby wave trains over mid-latitude regions of Eurasia.

Conflict of Interest

The authors declare no conflicts of interest relevant to this study.

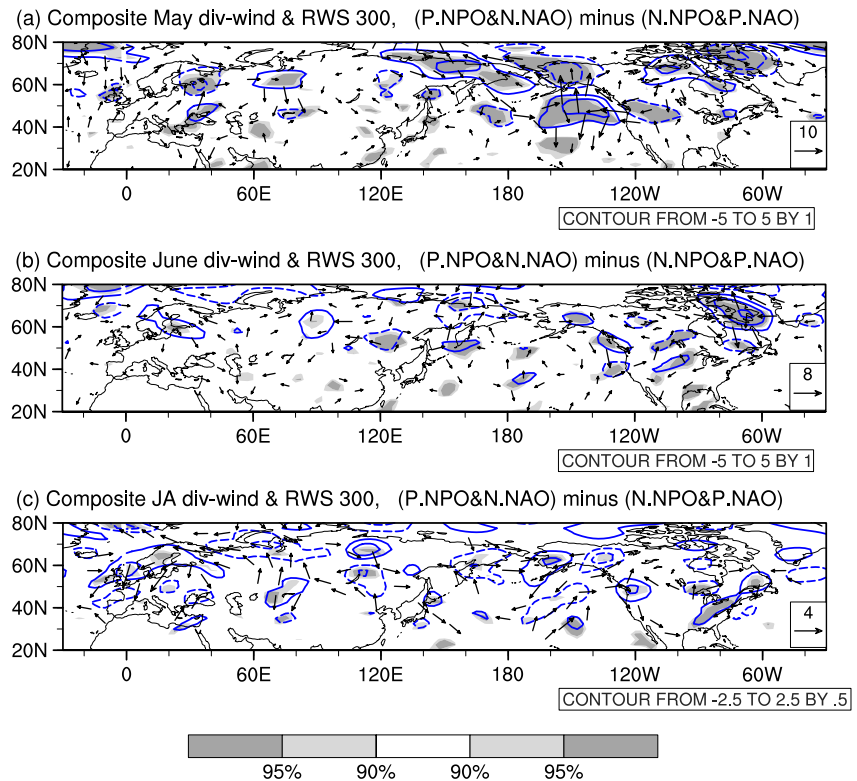


Figure 13. Differences in 300-hPa Rossby wave source (contours, $10^{-9}/s^2$) and divergent wind component (vectors, m/s) anomalies between the NPO+/NAO- and NPO-/NAO+ years during the period of significant NPO–Precip_{NEC} relationship: (a, b) May, (c, d) June, and (e, f) midsummer. Dark (light) shadings indicate Rossby wave source anomalies that significantly exceed the 95% (90%) confidence level, estimated using Student's *t*-test. Vectors with magnitude of <2.0 are not plotted.

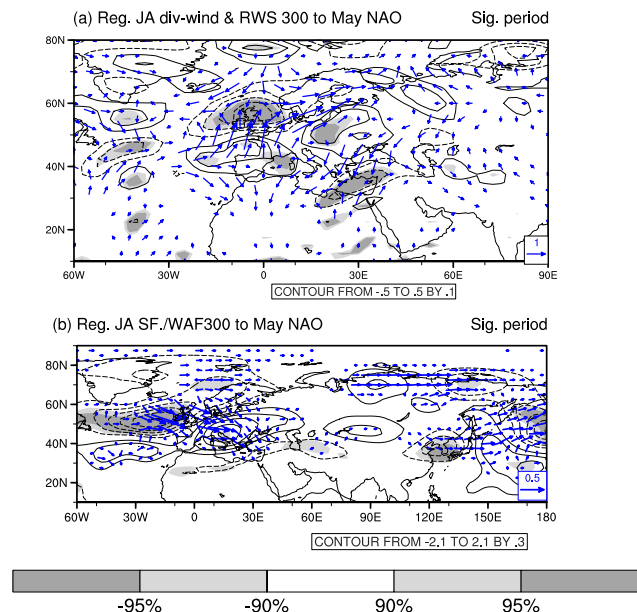


Figure 14. Midsummer (a) Rossby wave source (contours, $10^{-9}/s^2$) and divergent wind component (vectors, m/s) and (b) streamfunction (contours, 10^6 m²/s) and wave activity flux (vectors, m²/s²) anomalies at 300 hPa regressed against the May NAO index during the period of significant NPO–Precip_{NEC} relationship. Dark (light) shadings indicate Rossby wave source anomalies in (a) and streamfunction anomalies in (b) that significantly exceed the 95% (90%) confidence level, estimated using the Student's *t*-test. Vectors with magnitude of <0.2 in (a) are not plotted. Vectors with magnitude of <0.05 in (b) are not plotted.

Data Availability Statement

The precipitation records [Dataset] (Wu & Gao, 2013) are obtained from CN05 dataset. The NCEP/NCAR reanalysis data [Dataset] (Kalnay et al., 1996) are provided by the NOAA Physical Sciences Laboratory. The NAO index [Dataset] is derived from the Climate Prediction Center: <https://www.cpc.ncep.noaa.gov/products/precip/CWlink/pna/nao.shtml>.

Acknowledgments

We sincerely acknowledge the Editor, Associate Editor and two anonymous reviewers whose kind and valuable comments greatly improved the quality of this manuscript. This work was jointly supported by Guangdong Major Project of Basic and Applied Basic Research (Grant 2020B0301030004) and the National Natural Science Foundation of China (Grants 42075030 and 41875119).

References

- Ao, J., & Sun, J. Q. (2016). Decadal change in factors affecting winter precipitation over eastern China. *Climate Dynamics*, *46*(1–2), 111–121. <https://doi.org/10.1007/s00382-015-2572-7>
- Chen, D., Gao, Y., Sun, J. Q., Wang, H. J., & Ma, J. H. (2020). Interdecadal variation and causes of drought in Northeast China in recent decades. *Journal of Geophysical Research: Atmospheres*, *125*(17), e2019JD032069. <https://doi.org/10.1029/2019JD032069>
- Chen, D., Sun, J. Q., & Gao, Y. (2019). Distinct impact of the Pacific multi-decadal oscillation on precipitation in Northeast China during April in different Pacific multi-decadal oscillation phases. *International Journal of Climatology*, *40*(3), 1–14. <https://doi.org/10.1002/joc.6291>
- Chen, D., Wang, H. J., Liu, J. P., & Li, G. P. (2015). Why the spring North Pacific Oscillation is a predictor of typhoon activity over the western North Pacific. *International Journal of Climatology*, *35*(11), 3353–3361. <https://doi.org/10.1002/joc.4213>
- Chen, S. F., & Wu, R. G. (2018). Impacts of winter NPO on subsequent winter ENSO: Sensitivity to the definition of NPO index. *Climate Dynamics*, *50*(1–2), 375–389. <https://doi.org/10.1007/s00382-017-3615-z>
- Choi, K. S., Oh, S. B., Byun, H. R., Kripalani, R. H., & Kim, D. W. (2011). Possible linkage between East Asian summer drought and North Pacific Oscillation. *Theoretical and Applied Climatology*, *103*(1–2), 81–93. <https://doi.org/10.1007/s00704-010-0286-7>
- Guo, D., & Sun, Z. B. (2004). Relationships of winter North Pacific Oscillation anomalies with the East Asian winter monsoon and the weather and climate in China (in Chinese). *Journal of Nanjing Institute Meteorology*, *27*, 461–470.
- Han, T. T., Chen, H. P., & Wang, H. J. (2015). Recent changes in summer precipitation in Northeast China and the background circulation. *International Journal of Climatology*, *35*(14), 4210–4219. <https://doi.org/10.1002/joc.4280>
- Han, T. T., He, S. P., Hao, X., & Wang, H. J. (2018). Recent interdecadal shift in the relationship between Northeast China's winter precipitation and the North Atlantic and Indian Oceans. *Climate Dynamics*, *50*(3–4), 1413–1424. <https://doi.org/10.1007/s00382-017-3694-x>
- Han, T. T., Wang, H. J., Hao, X., & Li, S. F. (2019). Seasonal prediction of midsummer extreme precipitation days over Northeast China. *Journal of Applied Meteorology and Climatology*, *58*(9), 2033–2048. <https://doi.org/10.1175/JAMC-D-18-0253.1>
- Han, T. T., Wang, H. J., & Sun, J. Q. (2017). Strengthened relationship between eastern ENSO and summer precipitation over Northeast China. *Journal of Climate*, *30*(12), 4497–4512. <https://doi.org/10.1175/JCLI-D-16-0551.1>
- Han, T. T., Zhang, M. H., Zhou, B. T., Hao, X., & Li, S. F. (2020). Strengthened relationship between tropical West Pacific and midsummer precipitation over Northeast China after the mid-1990s. *Journal of Climate*, *33*(16), 6833–6848. <https://doi.org/10.1175/JCLI-D-19-0957.1>
- Hu, Y. P., Zhou, B. T., Han, T. T., & Li, H. X. (2023). Enhanced linkage of summer drought in southern China to the North Pacific Oscillation since 2000. *Journal of Geophysical Research: Atmospheres*, *128*(4), e2022JD037432. <https://doi.org/10.1029/2022JD037432>
- Kalnay, E., Kanamitsu, M., Kistler, R., Collins, W., Deaven, D., Gandin, L., et al. (1996). The NCEP/NCAR 40-year reanalysis project [Dataset]. *Bulletin of the American Meteorological Society*, *77*(3), 437–471. [https://doi.org/10.1175/1520-0477\(1996\)077<0437:TNYRP>2.0.CO;2](https://doi.org/10.1175/1520-0477(1996)077<0437:TNYRP>2.0.CO;2)
- Li, C. Y., & Li, G. L. (2000). The NPO/NAO and interdecadal climate variations in China. *Advances in Atmospheric Sciences*, *17*(4), 555–561. <https://doi.org/10.1007/s00376-000-0018-5>
- Lian, Y., Shen, B. Z., Li, S. F., Zhao, B., Gao, Z. T., Liu, G., et al. (2013). Impacts of polar vortex, NPO, and SST configurations on unusually cool summers in Northeast China. Part I: Analysis and diagnosis. *Advances in Atmospheric Sciences*, *30*(1), 193–209. <https://doi.org/10.1007/s00376-012-1258-x>
- Linkin, M. E., & Nigam, S. (2008). The North Pacific Oscillation–West Pacific teleconnection pattern: Mature-phase structure and winter impacts. *Journal of Climate*, *21*(9), 1979–1997. <https://doi.org/10.1175/2007JCLI2048.1>
- Park, C. K., Ho, C. H., Park, D. S. R., Park, T. W., & Kim, J. (2020). Interannual variations of spring drought-prone conditions over three subregions of East Asia and associated large-scale circulations. *Theoretical and Applied Climatology*, *142*(3–4), 1117–1131. <https://doi.org/10.1007/s00704-020-03371-5>
- Park, G., Park, Y. H., Vivier, F., Kwon, Y. O., & Chang, K. I. (2014). Regime-dependent nonstationary relationship between the East Asian winter monsoon and North Pacific Oscillation. *Journal of Climate*, *27*(21), 8185–8204. <https://doi.org/10.1175/JCLI-D-13-00500.1>
- Plumb, R. A. (1985). On the three-dimensional propagation of stationary waves. *Journal of the Atmospheric Sciences*, *42*(3), 217–229. [https://doi.org/10.1175/1520-0469\(1985\)042<0217:OTTDPO>2.0.CO;2](https://doi.org/10.1175/1520-0469(1985)042<0217:OTTDPO>2.0.CO;2)
- Rogers, J. C. (1981). The North Pacific Oscillation. *Journal of Climatology*, *1*, 39–57. <https://doi.org/10.1002/joc.3370010106>
- Sardeshmukh, P. D., & Hoskins, B. J. (1988). The generation of global rotational flow by steady idealized tropical divergence. *Journal of the Atmospheric Sciences*, *45*(7), 1228–1251. [https://doi.org/10.1175/1520-0469\(1988\)045<1228:TGOGRF>2.0.CO;2](https://doi.org/10.1175/1520-0469(1988)045<1228:TGOGRF>2.0.CO;2)
- Shen, B. Z., Lin, Z. D., Lu, R. Y., & Lian, Y. (2011). Circulation anomalies associated with interannual variation of early- and late-summer precipitation in Northeast China. *Science China Earth Sciences*, *54*(7), 1095–1104. <https://doi.org/10.1007/s11430-011-4173-6>
- Song, L. Y., Chen, S. F., Chen, W., Duan, W. S., & Li, Y. (2021). Interdecadal change in the relationship between boreal winter North Pacific Oscillation and Eastern Australian rainfall in the following autumn. *Climate Dynamics*, *57*(11–12), 3265–3283. <https://doi.org/10.1007/s00382-021-05864-z>
- Sun, J. Q., Wang, H. J., & Yuan, W. (2008). Decadal variations of the relationship between the summer North Atlantic Oscillation and Middle East Asian air temperature. *Journal of Geophysical Research*, *113*(D15), D15107. <https://doi.org/10.1029/2007JD009626>
- Sun, L., Shen, B. Z., Sui, B., & Huang, B. (2017). The influences of East Asian monsoon on summer precipitation in Northeast China. *Climate Dynamics*, *48*(5–6), 1647–1659. <https://doi.org/10.1007/s00382-016-3165-9>
- Sung, M. K., Jang, H. Y., Kim, B. M., Yeh, S. W., Choi, Y. S., & Yoo, C. (2019). Tropical influence on the North Pacific Oscillation drives winter extremes in North America. *Nature Climate Change*, *9*(5), 413–418. <https://doi.org/10.1038/s41558-019-0461-5>
- Tseng, Y. H., Ding, R. Q., Zhao, S., Kuo, Y. C., & Liang, Y. C. (2020). Could the North Pacific Oscillation be modified by the initiation of the East Asian winter monsoon? *Journal of Climate*, *33*(6), 2389–2406. <https://doi.org/10.1175/JCLI-D-19-0112.1>
- Vimont, D. J., Battisti, D. S., & Hirst, A. C. (2001). Foot-printing: A seasonal connection between the tropics and mid-latitudes. *Geophysical Research Letters*, *28*(20), 3923–3926. <https://doi.org/10.1029/2001GL013435>
- Walker, G. T., & Bliss, E. W. (1932). World weather V. *Memoirs of the Royal Meteorological Society*, *4*, 53.

- Wallace, J. M., & Gutzler, D. S. (1981). Teleconnections in the geopotential height field during the Northern Hemisphere winter. *Monthly Weather Review*, *109*(4), 784–812. [https://doi.org/10.1175/1520-0493\(1981\)109<0784:TITGHF>2.0.CO;2](https://doi.org/10.1175/1520-0493(1981)109<0784:TITGHF>2.0.CO;2)
- Wang, L., Chen, W., & Huang, R. H. (2007). Changes in the variability of North Pacific Oscillation around 1975/1976 and its relationship with East Asian winter climate. *Journal of Geophysical Research*, *112*(D11), D11110. <https://doi.org/10.1029/2006JD008054>
- Wu, J., & Gao, X. J. (2013). A gridded daily observation dataset over China region and comparison with the other datasets (in Chinese) [Dataset]. *Chinese Journal of Geophysics*, *56*, 1102–1111. <https://doi.org/10.6038/cjg20130406>
- Zhang, L. X., Wu, P. L., Zhou, T. J., & Xiao, C. (2018). ENSO transition from La Niña to El Niño drives prolonged spring–summer drought over North China. *Journal of Climate*, *31*(9), 3509–3523. <https://doi.org/10.1175/JCLI-D-17-0440.1>
- Zhou, B. T., & Xia, D. D. (2012). Interdecadal change of the connection between winter North Pacific Oscillation and summer precipitation in the Huaihe River valley. *Science China Earth Sciences*, *55*(12), 2049–2057. <https://doi.org/10.1007/s11430-012-4499-8>
- Zhou, M. Z., & Wang, H. J. (2014). Late winter sea ice in the Bering Sea: Predictor for maize and rice production in Northeast China. *Journal of Applied Meteorology and Climatology*, *53*(5), 1183–1192. <https://doi.org/10.1175/JAMC-D-13-0242.1>
- Zhu, Y. L. (2011). A seasonal prediction model for the summer rainfall in Northeast China using the year-to-year increment approach. *Atmospheric and Oceanic Science Letters*, *4*(3), 146–150. <https://doi.org/10.1080/16742834.2011.11446920>